Hindawi
International Journal of Antennas and Propagation
Volume 2019, Article ID 6732758, 8 pages
https://doi.org/10.1155/2019/6732758

Research Article

Ultra-Wideband Dielectric Lens Antennas for Beamsteering Systems

Renan Alves dos Santos,[1] **Gabriel Lobão da Silva Fré**,[2] **Luís Gustavo da Silva**,[3] **Marcelo Carneiro de Paiva**,[3] **and Danilo Henrique Spadoti**[2]

[1]*Faculty of Electrical Engineering, Federal University of Uberlândia (UFU), Padre Pavoni Street 294, 38701-002 Patos de Minas, Minas Gerais, Brazil*
[2]*Federal University of Itajubá (UNIFEI), Benedito Pereira dos Santos Avenue 1303, 37500-903 Itajubá, Minas Gerais, Brazil*
[3]*Inatel Competence Center, National Institute of Telecommunications (INATEL), João de Camargo Avenue 510, 37540-000 Santa Rita do Sapucaí, Minas Gerais, Brazil*

Correspondence should be addressed to Renan Alves dos Santos; renans@ufu.br

Received 15 April 2019; Revised 10 June 2019; Accepted 28 June 2019; Published 6 August 2019

Academic Editor: Giorgio Montisci

This paper presents a high-directivity ultra-wideband beamsteering antenna array. An innovative beamsteering system based on hemispherical dielectric lenses fed by a set of different printed antennas is proposed. Diversity of signals in different spatial positions can be radiated at the same time. A prototype was manufactured and characterized, operating in a bandwidth varying from 8 GHz to 12 GHz with gain up to 13 dBi.

1. Introduction

Wireless communication systems are constantly evolving, driven by new proposals, such as the fifth-generation mobile communications system (5G) [1–4], Internet of things (IoT) [5–7], among others. Moreover, the exponential increase of mobile data traffic is challenging global researchers to propose new devices and technologies, since the current scenario will be unable to satisfy such expected demand.

According to Shannon's information theory [8], there are two ways to meet the growing data rate demands: either by increasing signal bandwidth or increasing the signal-to-noise ratio (SNR). Looking to the wireless communication systems, one of the main components that limit the speed of the data rate is the antennas, once is just a conventional passive radiator element. Therefore, antennas applied for the future telecommunication networks are expected to present high gain in a broadband frequency range and a reconfigurable radiation pattern [9–12]. Thus, there is a great interest in working with more directive radiators, which allows the signal-to-noise ratio at the receiver to be increased. This concept is being reached by system proposals with radiation pattern control [13, 14]. These systems can be summarized as a multiple antenna array that allows for radiated beam variation from a feeding phase control of each radiator element.

In conventional systems with variable irradiated beams, i.e. beamsteering, a single signal is applied to each array antenna. Therefore, the beamsteering is a result of the time delay between these signals, reconfiguring the structure radiation pattern, but with great restraint since the output signal is always the same. As a solution to this limitation, there are several works on lens antennas for beamsteering systems [15–17]. The lens antennas advantage is that with only a single feeder, if the design is correctly executed such a directive structure as an antennas array is achieved. In addition, just by varying the position of the feeder relative to the center of the lens produces the beamsteering.

It is possible to attend the need for high directivity and beamsteering with wideband operation using dielectric lens antennas [18, 19]. In [18], a spherical lens was fed by an antipodal Fermi tapered slot antenna array to obtain

beamsteering at a bandwidth of 33.3%. In [19], a Luneburg lens based on a 2D parallel-plate structure was fed by probe pins periodically arranged in a circle obtaining beamsteering at a bandwidth of 24.1%. The studies presented in [8, 9] also have the capability to beamsteering over a large bandwidth, however, using a complex lens or feeder structure.

In this paper, a hemispherical dielectric lens is fed by an ultra-wideband printed antenna array (Figure 1) to obtain beamsteering at a bandwidth of 40%. The proposed structure offers a diversity of applications, with high gain in an ultra-wideband, with a simple structure design.

2. Ultra-Wideband Printed Antenna Design

The ultra-wideband operation was achieved using a microstrip antenna (MsA). The first step was to reduce MsA's ground plane by turning it into a printed monopole antenna [20]. The second step was to round the vertices at the patch bottom, transforming the printed monopole antenna in ultra-wideband printed antenna [20]. The design starts with a microstrip antenna dimensioning to operate at 10 GHz. A SMA connector was inserted into the feedline to minimize undesirable parasitic effects. The MsA dimensions are carefully calculated and adjusted to minimize the input reflection. The optimized parameters detailed in Figure 2(a) are patch width $W = 12.9$ mm and length $L = 9.6$ mm, the impedance matching slots width $\omega_c = 0.52$ mm and length $x_c = 3.2$ mm, and feedline width $\omega_l = 3.1$ mm and length $L_\ell = 2.13$ mm, in a substrate thickness $h = 1.52$ mm.

The MsA simulated reflection coefficient, S_{11}, of the input port is plotted in Figure 3(a). The optimized bandwidth varyies from 9.75 to 10.25 GHz for $S_{11} < -10$ dB (5%). The reduction in the ground plane decreases the MsA merit factor, increasing the bandwidth. The printed monopole antenna (see Figure 2(b)) has no impedance-matching slots. The slots act as a narrowband impedance matching device impairing the ultra-wideband antenna's behavior.

The printed monopole antenna bandwidth widening was investigated in terms of the ground plane length (L_t). The printed monopole antenna reflection coefficient was simulated and the results for different L_t are plotted in Figure 3(a). This antenna operates from 6.92 to 11.1 GHz for $L_t = L_\ell = 3.2$ mm, increasing fractionate bandwidth by 46.4%.

A smooth impedance transition between the feedline and the patch is guaranteed by the rounding vertices, eliminating the charge concentration. Thus, an improvement in both the impedance matching and in the broadband operation was achieved.

Ultra-wideband printed antenna (see Figure 2(c)) was investigated in terms of the rounding radius (ρ). The radius $\rho = 0$ mm refers to the patch without any rounding. The increment in ρ was done in function of the width W. The simulated reflection coefficient of the input port was plotted in Figure 3(b). In principle, increasing the ρ size, a significant improvement was observed not only in the S_{11} but also in the antenna band widening. As a result, the antenna largest bandwidth operates from 6.8 to 12.86 GHz for $\rho = 0.3$, $W = 3.87$ mm, increasing fractionate bandwidth by 61.65%.

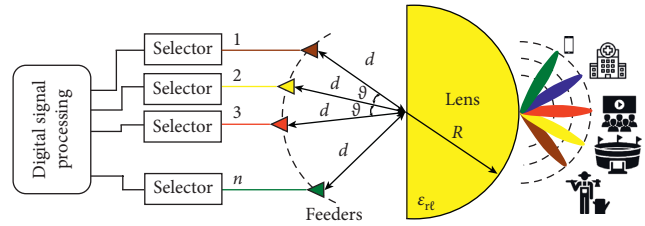

Figure 1: Beamsteering system proposed.

The radiation pattern is shown in Figure 4 for the ultra-wideband printed antenna ($L_t = 3.2$ mm and $\rho = 3.87$ mm) for the frequencies $f = 7$, 10, and 13 GHz, in black, red, and blue curves, respectively. It is possible to note that the gain is 2 dBi (7 GHz), 4 dBi (10 GHz), and 3 dBi (13 GHz), respectively. The ground plane acts as a director, i.e., the maximum radiation occurs for $\vartheta = 180^\circ$. The ground plane reduction modifies the radiation format, compared with a conventional microstrip antenna. However, the ground plane reduction guarantees ultra-wideband operation. The antenna operates with a radiation pattern similar to a half wavelength dipole at 10 GHz (omnidirectional in the xz-plane and with two nulls in the yz-plane). However, the surface current distribution in the patch deforms the radiated fields especially in the band limit (7 GHz and 13 GHz).

3. Ultra-Wideband Dielectric Lens Antennas for Beamsteering Systems

A device with a hemispherical dielectric lens fed with an ultra-wideband printed antenna ($L_t = 3.2$ mm and $\rho = 3.87$ mm) was designed to increase the gain. Operation in microwave frequency ranges requires appropriate lens material to avoid electromagnetic impairments, such as attenuation, fading, among others. The lens was built with polytetrafluoroethylene polymer (PTFE) with low dielectric losses in the microwave frequency range. Moreover, the design of the hemispherical dielectric lens antenna (see Figure 1) involves two main variables: the distance between the feeders and the flat surface of the lens (d) and the lens radius (R) [21, 22]. The d value indicates the focal point in which the feeder should be positioned. As present in [20], the d value represents the correct distance between the feeders and the flat surface of the lens, in which the lens can efficiently work as an energy collimator. The radius $R = 90$ mm was chosen to facilitate the manufacturing process, and the d value can be determined from [21] as follows:

$$d = \left(\frac{\sqrt{\varepsilon_{re}}}{\sqrt{\varepsilon_{rl}} - \sqrt{\varepsilon_{re}}} - 1 \right) R, \quad (1)$$

where ε_{rl} and ε_{re} are the lens dielectric permittivity, and the external medium dielectric permittivity, respectively.

For the design of the hemispherical dielectric lens, we used polytetrafluoroethylene (PTFE) material with $\varepsilon_{r\ell} = 2.2$ and radius $R = 3\lambda_0$ at 10 GHz ($R = 90$ mm), where λ_0 is the wavelength in the free space, and the external medium is a vacuum, resulting in a $d = 96.24$ mm. The ultra-wideband

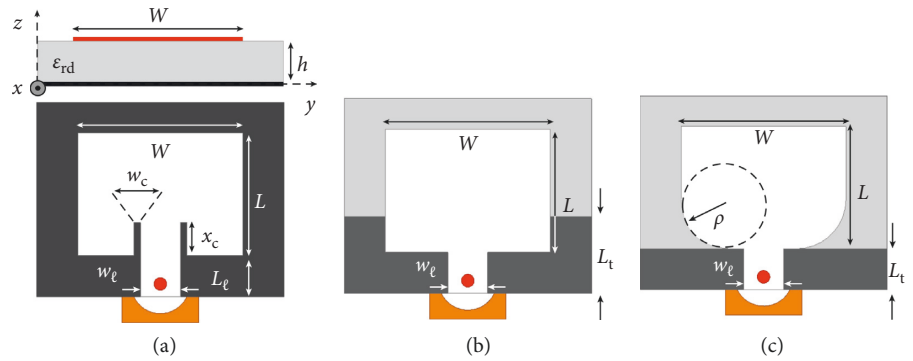

FIGURE 2: Printed antennas modifications: (a) microstrip antenna, (b) printed monopole antenna, and (c) ultra-wideband printed antenna.

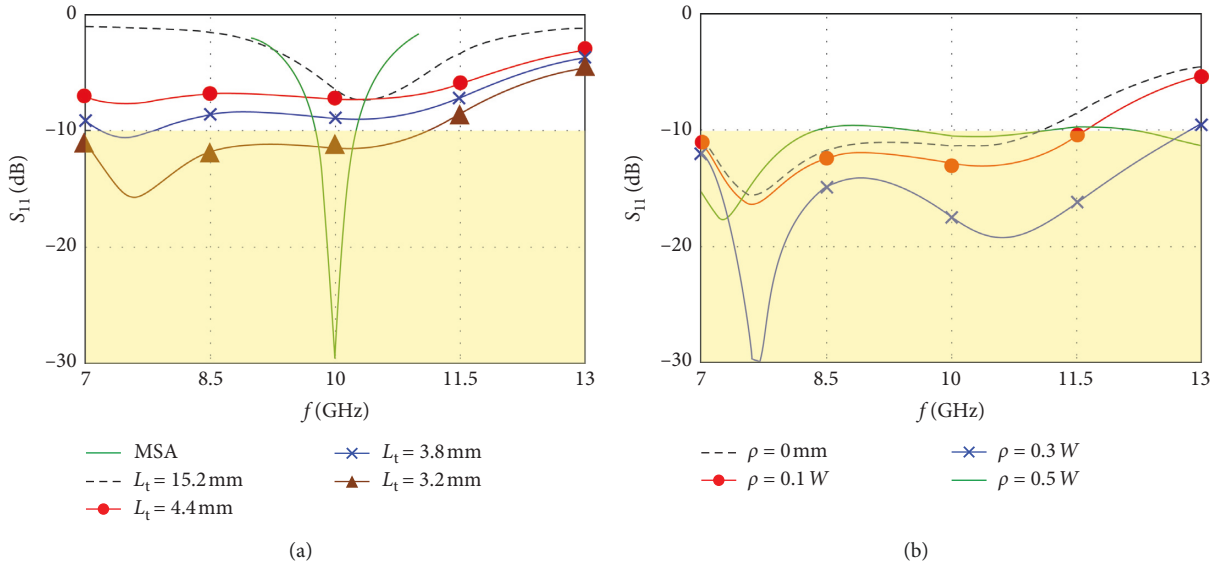

FIGURE 3: Printed antenna bandwidth widening study. (a) Ground plane reduction. (b) Patch bottom vertices rounding.

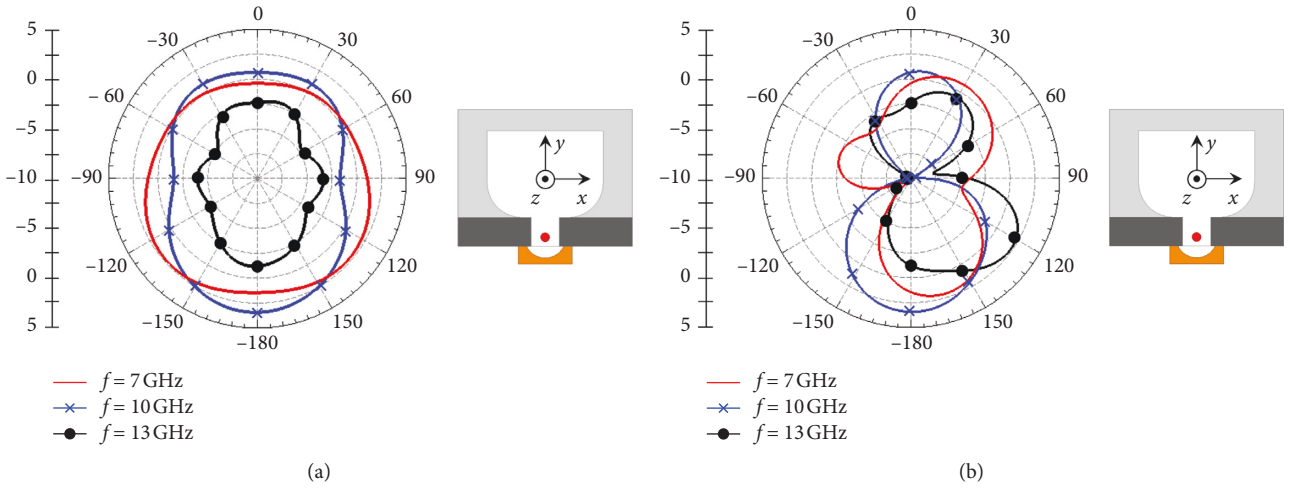

FIGURE 4: Radiation pattern for the ultra-wideband printed antenna. (a) *xz*-plane; (b) *yz*-plane.

printed antenna results in a wide bandwidth in terms of its reflection coefficient (S_{11}). Consequently, it is important to investigate the impact on lens impedance matching, as well as the formation of radiation throughout the bandwidth.

3.1. Impact of Lens and Mutual Coupling between Illuminators in S_{11}. Figure 5 shows the reflection coefficient (numerically calculated by ANSYS HFSS) considering a scenario with three angled illuminators, with variation of $\vartheta = 20^{\circ}$, as shown in Figure 1. The mutual coupling among the feeders, as well as the reflections, that occur in the transition between the air and lens causes these small variations in the S_{11} curves. However, the reflection coefficient frequency response (presented in Figure 5) shows good similarity when compared with the S_{11} with only one ultra-wideband printed antenna. Therefore, the existence of the lens and the presence of more than one feeder do not significantly impair the S_{11}.

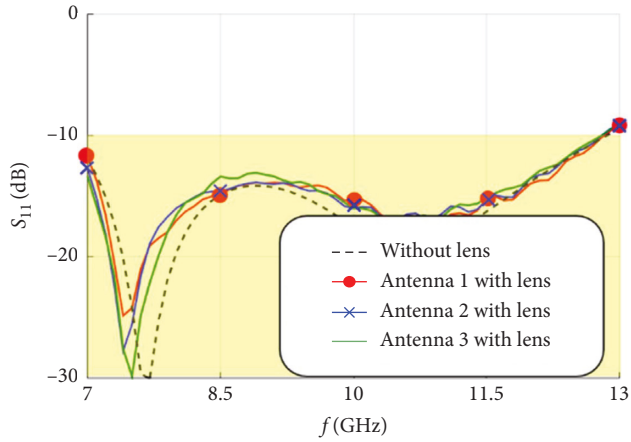

Figure 5: Influence of mutual coupling among feeders and reflections that occur in the transition between air and lens in the reflection coefficient.

3.2. Formation of Radiation throughout the Bandwidth. In addition to the S_{11} values, it is important to study the behavior of the radiated fields. In this project, the function of the lens was to collimate the energy that comes from the feeder converting it into a nonhomogenous plane-wave (with the same phase, but with different amplitude). Thus, Figure 6 shows the electric field magnitude for three frequencies: 7 GHz, 10 GHz, and $f = 13$ GHz. These frequencies were chosen to study the wavefront formation at the beginning, middle, and end bandwidth ranges.

For $f = 7$ GHz (Figure 6(a)), the lens diameter relative to the wavelength is $d = 4.08\lambda_0$, i.e., electrically smaller than 10 GHz. Therefore, resonance effects can occur inside the dielectric material [23]. This effect was highlighted by the white dotted curve, in Figure 6(a). However, since the lens diameter is greater than λ_0, the lens output is still in equiphase. For $f = 10$ GHz, a resonance intensity reduction occurred indicating small perturbation in the radiation, thereby keeping a plane wavefront. For $f = 13$ GHz, a leakage of energy at the lens edges occurred, as shown by the white dotted curve, in Figure 6(c). For higher frequencies, the ultra-wideband printed antenna tends to drive the energy to a position outside of the lens's capture area. As a result, undesirable effects occur but do not affect the output equiphase radiation wavefront.

By analyzing the reflection coefficient and the radiated field distribution, the antenna bandwidth was defined between 8 GHz $\leq f \leq$ 12 GHz, with a fractional band of operation Bw = 40%, in relation to the central frequency $f = 10$ GHz.

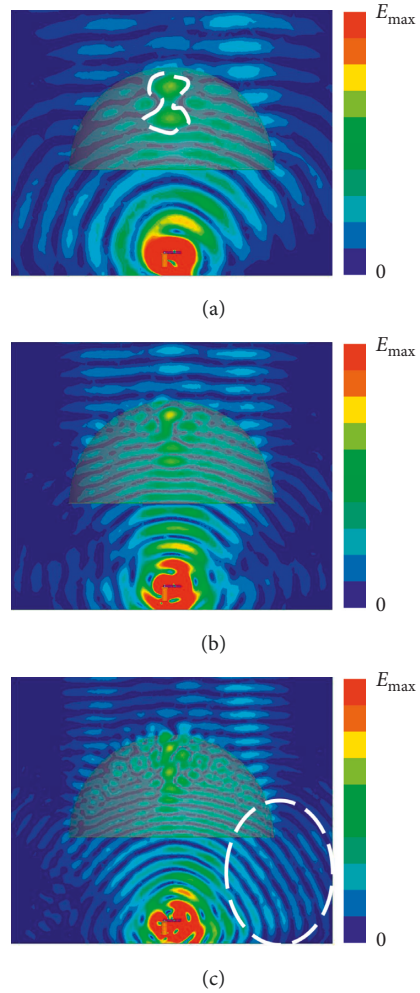

Figure 6: Ultra-wideband dielectric lens electric field magnitude analysis. (a) $f = 7.0$ GHz, (b) $f = 10.0$ GHz, and (c) $f = 13.0$ GHz.

4. Results and Discussion

An experimental setup was developed, as shown in Figure 7, with three ultra-wideband printed antenna as feeders. Then, a device was designed for the lens mechanical suspension composed of a wooden base (brown), with relative dielectric permittivity and dissipation factor, $\varepsilon_{rw} = 1.22$ and $\tan(\delta)_w = 0.1$, respectively [24]. Polylactic (PLA) supports were used for the lens, feeder position, and alignment (in gray color), with $\varepsilon_{rs} = 2.79$ and $\tan(\delta)_s = 0.2$ [25]. To improve the lens support, a cylindrical extension was designed, with length $d_s = 20$ mm

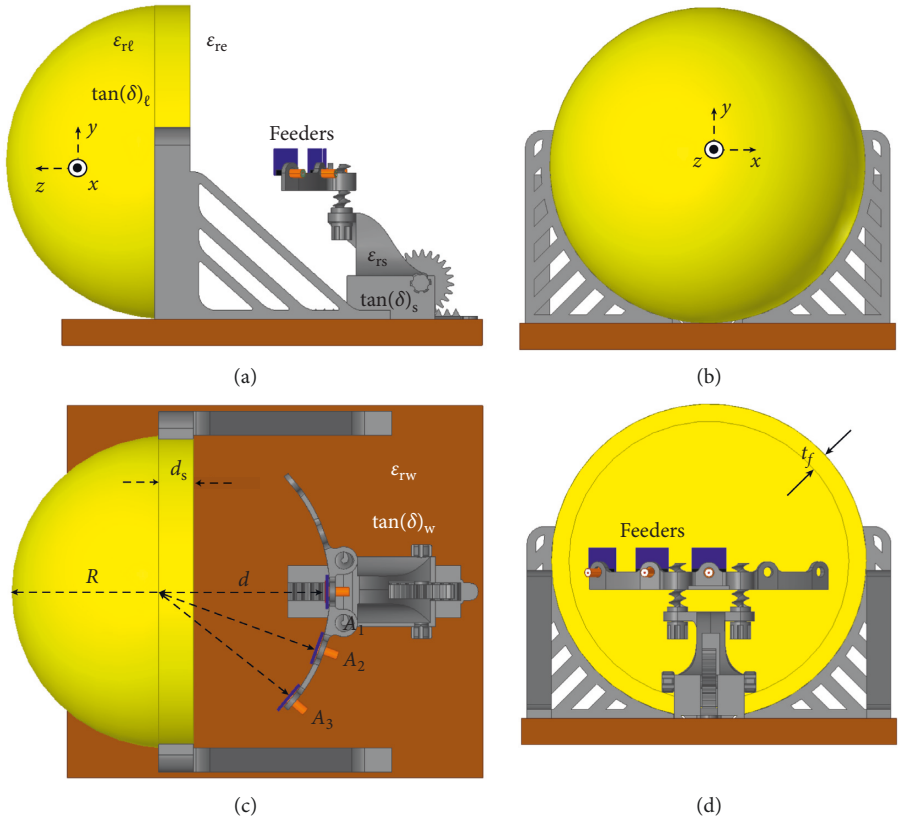

FIGURE 7: Model of the ultra-wideband dielectric lens antenna for beamsteering systems. (a) Side view. (b) Front view. (c) Upper view. (d) Back view.

and width $t_s = 10$ mm (see Figure 6(c)). The device configuration was studied in the ANSYS HFSS in order to cause the least prejudicial influence possible in the operation of the structure. The device configuration was studied in the ANSYS HFSS in order to cause the least prejudicial influence possible in the operation of the structure. The mounting bracket geometry was studied to minimize undesirable influences in the impedance matching and radiation pattern. So, a prototype for ultra-wideband dielectric lens antenna for beamsteering system was constructed (see final experimental setup in Figure 8).

4.1. Reflection Coefficient. Figure 9 shows the simulated and measured S_{11} curves of the proposed hemispherical dielectric lens antenna. The measured and simulated curves are very similar. The small variations between the curves are credited mainly to manufacturing errors and fluctuations in material properties. However, the prototype continues to have a bandwidth of 40% ($8\,\text{GHz} \leq f \leq 12\,\text{GHz}$).

4.2. Radiation Performance. As presented in [21], when the primary feeders have a wide beam radiation pattern, there is an energy overflow at the lens edges. This directly impacts the lens aperture efficiency, reducing directivity, and consequently reducing the gain. According to [21], using a directional horn antenna, the maximum aperture efficiency for PTFE lens is 59%. However, illuminating this lens with a broadband printed antenna as feeder the maximum aperture efficiency obtained is 42%, due to the wide beam radiation pattern.

Even with the reduction in the lens aperture efficiency due to the omnidirectional radiation pattern, we chose to use a printed antenna to guarantee its main advantage, i.e., ultralarge bandwidth operation. This is the main reason for choosing this feeder for the design.

The reconfigurable radiation patterns with three ultra-wideband printed antennas, angled in 20° between each antenna, were simulated and measured (see Figure 10). Antenna 1 (A_1) had $\vartheta = 0°$, antenna 2 (A_2) had $\vartheta = 20°$, and antenna 3 (A_3) had $\vartheta = 40°$. The ANSYS HFSS simulation results were compared with experimental data for two different frequencies, $f = 8$ GHz and $f = 10$ GHz. These frequencies were chosen due to practical limitations, mainly because of the unavailability of a reference antenna operating above 10 GHz in our laboratory. The measured and simulated curves also showed extreme similarity. Again, the small variations between the curves can be credited to manufacturing errors and fluctuations in material properties. However, the prototype continues to present high gain, up to 13.0 dBi for $f = 8$ GHz and 13.3 dBi for $f = 10$ GHz.

4.3. Comparative Study. A comparative study of the proposed antenna with other preexisting literature designs of ultra-wideband dielectric lens antennas for beamsteering systems is presented in Table 1. We compared the structure complexity (lens or feeder), the lens radius, the gain in the

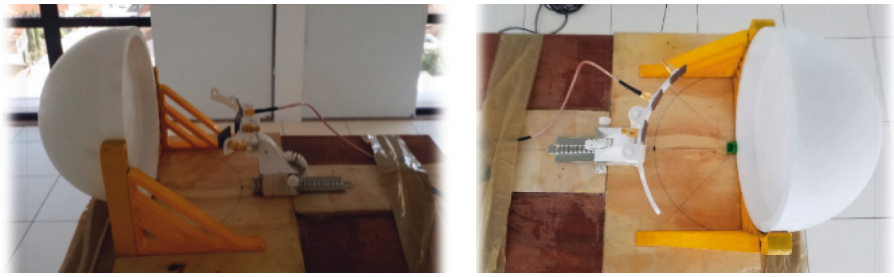

(a) (b)

Figure 8: Ultra-wideband dielectric lens antennas for beamsteering system prototype. (a) Side view. (b) Upper view.

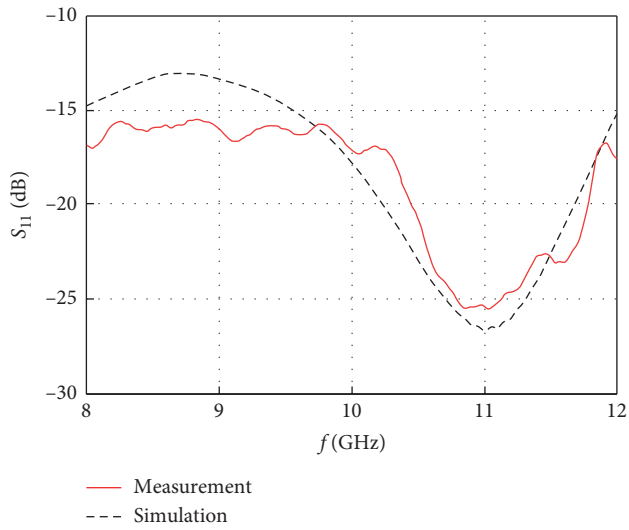

Figure 9: Reflection coefficient for an ultra-wideband dielectric lens antennas.

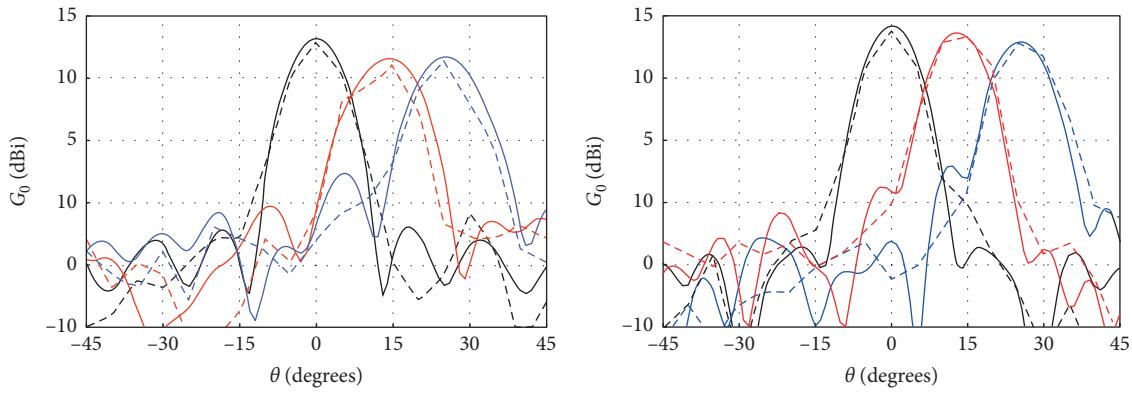

Figure 10: Ultra-wideband dielectric lens antennas for beamsteering system radiation pattern. —— A_1 simulation, - - - A_1 measurement, —— A_2 simulation, - - - A_2 measurement, —— A_3 simulation, - - - A_3 measurement. (a) $f = 8$ GHz; (b) $f = 10$ GHz.

direction of maximum radiation, and percentage bandwidth. The spherical lens [17] was designed with a radius of $2.4\lambda_0$. When fed by an antipodal Fermi tapered slot antenna array, a gain of 20.0 dBi and a bandwidth of 33.3% were achieved. The main disadvantage of this structure is the complexity of the feeders. The Fermi tapered slot antenna array is very small, which can make the design for certain frequencies very complicated. The parallel-plate Luneburg lens antenna [18] was designed with a radius of $3.6\lambda_0$. The authors achieved a gain of 14.5 dBi and a bandwidth of 24.1% when the antenna was fed by a probe pins. The main disadvantage of this structure is the complexity of the lens. The parallel-

Table 1: Comparisons with previous works of ultra-wideband dielectric lens antennas for beamsteering systems.

Reference	Structure	Lens radius (λ_0)	G_0 (dBi)	Bw (%)
[18]	Complex	2.4	20.0	33.3
[19]	Complex	3.6	14.5	24.1
This work	Simple	3.0	14.2	40.00

plate Luneburg lens has several dielectric layers, as well as two metal planes. Therefore, it is considerably complex and has high manufacturing cost. The design presented in this paper has similar results to those proposed in [18, 19]. However, there are some advantages: the feeders are compact, inexpensive, and easy to manufacture. Moreover, the dielectric lens is simple and homogeneous, presenting low cost and easy manufacturing (3D printer, for example). Additionally, the simpler structure of the set presents high gain in ultra-wideband with diversity of applications.

5. Conclusions

This paper numerically and experimentally investigated a directive, ultra-wideband, and reconfigurable system based on dielectric lens antennas for beamsteering operations. Simulated and measured results prove the structure's effectiveness. The bandwidth varies from 8 GHz to 12 GHz, and gain is greater than 13 dBi. Thus, the developed ultra-wideband dielectric lens antenna for beamsteering system could be an interesting solution to match the demands of future wireless communication systems.

Data Availability

The simulation and measurement data used to support the findings of this study are available from the corresponding author upon request.

Conflicts of Interest

The authors declare that they have no conflicts of interest.

Acknowledgments

This research was supported in part by the CAPES, CNPq, FAPEMIG, and Inatel Competence Center, National Institute of Telecommunications—INATEL, Brazil.

References

[1] X. Meng, J. Li, D. Zhou, and D. Yang, "5G technology requirements and related test environments for evaluation," *China Communications*, vol. 13, no. 2, pp. 42–51, 2016.

[2] L. Pierucci, "The quality of experience perspective toward 5G technology," *IEEE Wireless Communications*, vol. 22, no. 4, pp. 10–16, 2015.

[3] J. Lee, E. Tejedor, K. Ranta-aho et al., "Spectrum for 5G: global status, challenges, and enabling technologies," *IEEE Communications Magazine*, vol. 56, no. 3, pp. 12–18, 2018.

[4] N. Al-Falahy and O. Y. Alani, "Technologies for 5G networks: challenges and opportunities," *IT Professional*, vol. 19, no. 1, pp. 12–20, 2017.

[5] B. Hammi, R. Khatoun, S. Zeadally, A. Fayad, and L. Khoukhi, "IoT technologies for smart cities," *IET Networks*, vol. 7, no. 1, pp. 1–13, 2018.

[6] B. Xu, L. D. Xu, H. Cai, C. Xie, J. Hu, and F. Bu, "Ubiquitous data accessing method in IoT-based information system for emergency medical services," *IEEE Transactions on Industrial Informatics*, vol. 10, no. 2, pp. 1578–1586, 2014.

[7] S. M. R. Islam, D. Kwak, M. H. Kabir, M. Hossain, and K. S. Kwak, "The internet of things for health care: a comprehensive survey," *IEEE Access*, vol. 3, pp. 678–708, 2015.

[8] C. E. Shannon, "A mathematical theory of communication," *The Bell System Technical Journal*, vol. 27, pp. 379–423, 1948.

[9] S. X. Ta, H. Choo, and I. Park, "Broadband printed-dipole antenna and its arrays for 5G applications," *IEEE Antennas and Wireless Propagation Letters*, vol. 16, pp. 2183–2186, 2017.

[10] C. Lee, M. K. Khattak, and S. Kahng, "Wideband 5G beamforming printed array clutched by LTE-A 4 × 4-multiple-input–multiple-output antennas with high isolation," *IET Microwaves, Antennas & Propagation*, vol. 12, no. 8, pp. 1407–1413, 2018.

[11] M. M. M. Ali and A. R. Sebak, "Directive antennas for future 5G mobile wireless communications," in *Proceedings of the 2017 XXXIInd General Assembly and Scientific Symposium of the International Union of Radio Science (URSI GASS)*, pp. 1–4, IEEE, Montreal, QC, Canada, August 2017.

[12] M. R. D. Kodnoeih, Y. Letestu, R. Sauleau, E. M. Cruz, and A. Doll, "Compact folded fresnel zone plate lens antenna for mm-wave communications," *IEEE Antennas and Wireless Propagation Letters*, vol. 17, no. 5, pp. 873–876, 2018.

[13] M. V. Komandla, G. Mishra, and S. K. Sharma, "Investigations on dual slant polarized cavity-backed massive MIMO antenna panel with beamforming," *IEEE Transactions on Antennas and Propagation*, vol. 65, no. 12, pp. 6794–6799, 2017.

[14] M. Jiang, Z. N. Chen, Y. Zhang, W. Hong, and X. Xuan, "Metamaterial-based thin planar lens antenna for spatial beamforming and multibeam massive MIMO," *IEEE Transactions on Antennas and Propagation*, vol. 65, no. 2, pp. 464–472, 2017.

[15] Y. S. Zhang and W. Hong, "A millimeter-wave gain enhanced multi-beam antenna based on a coplanar cylindrical dielectric lens," *IEEE Transactions on Antennas and Propagation*, vol. 60, no. 7, pp. 3485–3488, 2012.

[16] J. G. Marin and J. Hesselbarth, "Lens antenna with planar focal surface for wide-angle beam-steering application," *IEEE Transactions on Antennas and Propagation*, vol. 67, no. 4, 2019.

[17] A. Boriskin, R. Sauleau, J. R. Costa, and C. Fernandes, "Integrated lens antennas," in *Aperture Antennas for Millimeter and Sub-millimeter Wave Applications*, A. Boriskin and R. Sauleau, Eds., Springer, Berlin, Germany, 2018.

[18] Z. Briqech, A.-R. Sebak, and T. A. Denidni, "Wide-scan MSC-AFTSA array-fed grooved spherical lens antenna for millimeter-wave MIMO applications," *IEEE Transactions on Antennas and Propagation*, vol. 64, no. 7, pp. 2971–2980, 2016.

[19] H.-T. Chou and Z.-D. Yan, "Parallel-plate Luneburg lens antenna for broadband multibeam radiation at millimeter-wave frequencies with design optimization," *IEEE Transactions on Antennas and Propagation*, vol. 66, no. 11, pp. 5794–5804, 2018.

[20] R. dos Santos, A. M. Muniz, M. Borsato, T. H. Brandão, T. N. Rodovalho, and S. A. Cerqueira, "Multi-technology wireless coverage based on a leaky-wave reconfigurable antenna," in *Proceedings of the 11th European Conference on*

Antennas and Propagation (EUCAP), pp. 2824–2828, Paris, France, March 2017.

[21] R. A. dos Santos, G. L. Fré, and D. H. Spadoti, "Technique for constructing hemispherical dielectric lens antennas," *Microwave and Optical Technology Letters*, vol. 61, no. 5, 2019.

[22] A. V. Boriskin, R. Sauleau, and A. I. Nosich, "Performance of hemielliptic dielectric lens antennas with optimal edge illumination," *IEEE Transactions on Antennas and Propagation*, vol. 57, no. 7, pp. 2193–2198, 2009.

[23] A. V. Boriskin, A. I. Nosich, S. V. Boriskina, T. M. Benson, P. Sewell, and A. Altintas, "Lens or resonator? electromagnetic behavior of an extended hemielliptic lens for a sub-millimeter-wave receiver," *Microwave and Optical Technology Letters*, vol. 43, no. 6, pp. 515–518, 2004.

[24] P. A. Rizzi, *Microwave Engineering: Passive Circuits*, Prentice-Hall, Upper Saddle River, NJ, USA, 1st edition, 1988.

[25] B. Riddle, J. Baker-Jarvis, and J. Krupka, "Complex permittivity measurements of common plastics over variable temperatures," *IEEE Transactions on Microwave Theory and Techniques*, vol. 51, no. 3, pp. 727–733, 2003.